



The Applications, Methodology and Characterization of Nano Ferrite

Dhiraj Meghe¹, Nandkishor Meshram², Jitendra Bhaiswar³, Samiksha Paunekar⁴,
Divya Lande⁵, Pallavi Toney⁶

^{1,3,4,5} Department of Physics, Nagpur Institute of Technology, Nagpur

² Department of Physics, Dr. Ambedkar College, Nagpur

⁶ Department of Physics, Saraswati Junior college, Nagpur

ABSTRACT

In the present era many researcher are focusing on Nano ferrites due to their exponentially diverse applications in catalysts, magnetic shielding, organic transformation, magnetic recording devices, electronic devices, medical devices, transformers care, information storage, microwave absorption and many more. This chapter focused on present state of Nano ferrites with different substitution along with their synthesis methodology, characterization and application. Synthesis of Nano ferrites by co-precipitation, solid state and sol-gel method and characterization to investigate structural, electrical, and magnetic and microwave absorption is also covered in the present chapter.

Key words: Nano ferrites, Zinc-cadmium Nano ferrites, Methodology, Characterization.

1. Introduction

Nano ferrite investigations is considered to be the most important area for researchers as it has lot of technological application. Since past few decades lot of research work is carried on the synthesis of novel magnetic materials in ferrites with new characterization such as structural, electrical, magnetic and microwave absorption. Basically, ferrites are materials composed of iron oxide and bivalent elements like Zn, Ni, Mn, Cu, Mg, Cd, etc. Ferromagnetic materials have an uneven magnitude of magnetic moment and opposite direction alignment when exposed to a magnetic field [1,2]. The advantage of ferrites include high permeability, high electrical resistivity, high temperature stability, wide frequency range, high saturation magnetization, low coactivity, low eddy current loss and low cast [2,4]. The ferrites are classified as a hard ferrites and soft ferrite. The soft ferrite is the ferromagnetic materials that are not able to hold their magnetism after magnetized. These materials are easily demagnetized and magnetized with a tiny hysteresis loop. They can be created by heating and slowly cooling them. The soft ferrites has high value of permeability and susceptibility and low value of eddy current losses retentivity coercivity. They are used in electro magnets, cores of transformer etc. [2,3]. After being magnetized, the hard ferrites are unique in that they can retain magnetism. These materials have a large hysteresis loop and are difficult to magnetize and demagnetize. They are created by heating and abruptly cooling. The hard ferrites have high value of retentivity, eddy current losses, coercitivity and low value of susceptibility and permeability. They are used in permanent magnet, loud speakers etc [2]. The spinel ferrites are the combination of oxides, silicates and germinate. The chemical composition of spinel ferrites is $M^{2+}Fe_2^{3+}O_4$ where M^{2+} represent divalent metal ions such as Mg, Mn, Ni, Zn, Co, etc., Fe_2^{3+} represent trivalent metal ions and O is oxygen. With two types of interstitial gaps for the metal ions—tetrahedral (A) sides and octahedral (B) sides—the oxygen ions in the spinel structure are securely bonded in a face-centered cubic lattice (FCC). Normal and inverse spinel structures make up the grouping of spinel ferrites. Trivalent ions fully fill the octahedral (B) sides of regular spinel, while the divalent metal ion



Chapter 4

(M^{2+}) fully occupies the tetrahedral (A) sites. The octahedral (B) side of an inverse spinel is entirely occupied by the divalent metal ion (M^{2+}), whereas the trivalent ions (Fe^{3+}) are equally distributed between the tetrahedral (A) and octahedral (B) sites. In these materials 8A sites and 16B sites are occupied by metallic ions [4,5,6,7,8,9,10]. The spinel ferrite have high electrical resistivity, moderate coercivity, low eddy current losses, [11,12], low melting point [13], chemical stability [14] and can be easily magnetized or demagnetized. The spinel ferrites finds application in medical devices, drug delivery [2], electronic device, catalyst, transformer core, digital tape, sensor and radio frequency application [11,12,13,14,15,16].

Three series, namely the iron-spinel, chromium-spinel, and aluminum-spinel series, can be used to divide the spinel gathering (Figure 1). The four types of aluminum spinel are galaxite ($MnAl_2O_4$), hercynite ($FeAl_2O_4$), gahnite ($ZnAl_2O_4$), and spinel ($MgAl_2O_4$). Aluminum spinel is utilized in the gem business because it is translucent, stronger, and less dense than other spinel. The mineral chromium spinel is a hard, metallic black oxide. The basic member of chromium spinel series is chromite ($FeCr_2O_4$) and another member is magnesiochromite ($MgCr_2O_4$). The iron-spinel (spinel ferrite) are hard, having low coercivity and black to brownish. The iron spinel is found as Trevorite ($NiFe_2O_4$), Cuprospinel ($CuFe_2O_4$), Magnesioferrite ($MgFe_2O_4$), Jacobsite ($MnFe_2O_4$), Magnetite (Fe_3O_4), [2].

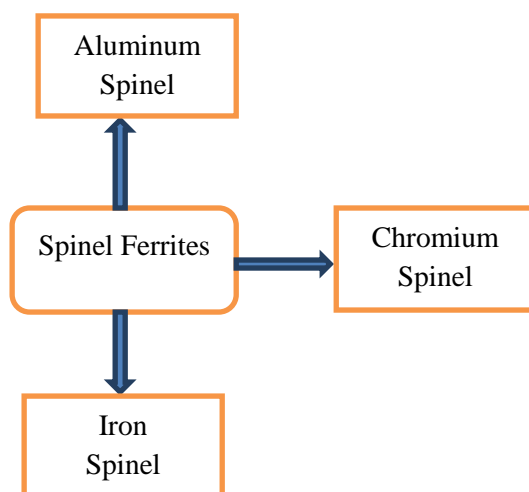


Figure 1. Types of spinel structure

2. SYNTHESIS OF NANO FERRITES

2.1 Sol Gel Method

The multi-step route known as "sol gel" includes chemical and physical steps related to polymerization, densification, gelation, condensation, drying, and hydrolysis. Figure 2 illustrates the ferrite manufacturing process using the sol gel method. Materials are extracted from chemical solutions by gelation in the sol gel process. There are two primary pathways: the inorganic pathway using metal salts in an aqueous solution (chloride, nitrate, oxychloride) and the metal-organic pathway using metal alkoxides in an organic solvent. Compared to metal alkoxides, the inorganic method is far less expensive and simpler to manage, but controlling the reactions is more challenging. More precise control over the phase formation, particle size homogeneity and intended stoichiometry are possible using the Sol Gel technique [17, 19]. Because it is less expensive, doesn't require specialized equipment, and can work at temperatures between 25 to 200°C—much lower than those of conventional solid-state reactions—the sol-gel technique is frequently used. Ferrites with exact morphologies, such as fibers, microspheres, and flower-like structures with a restricted size distribution, can be created using the sol-gel technique. The sol gel method has some drawbacks as well, including the need for expensive raw materials compared to high carbon content in the products, mineral-based metal ion sources, multiple steps, the need for close process monitoring, a lengthy processing time, and challenges with phase separation [18].

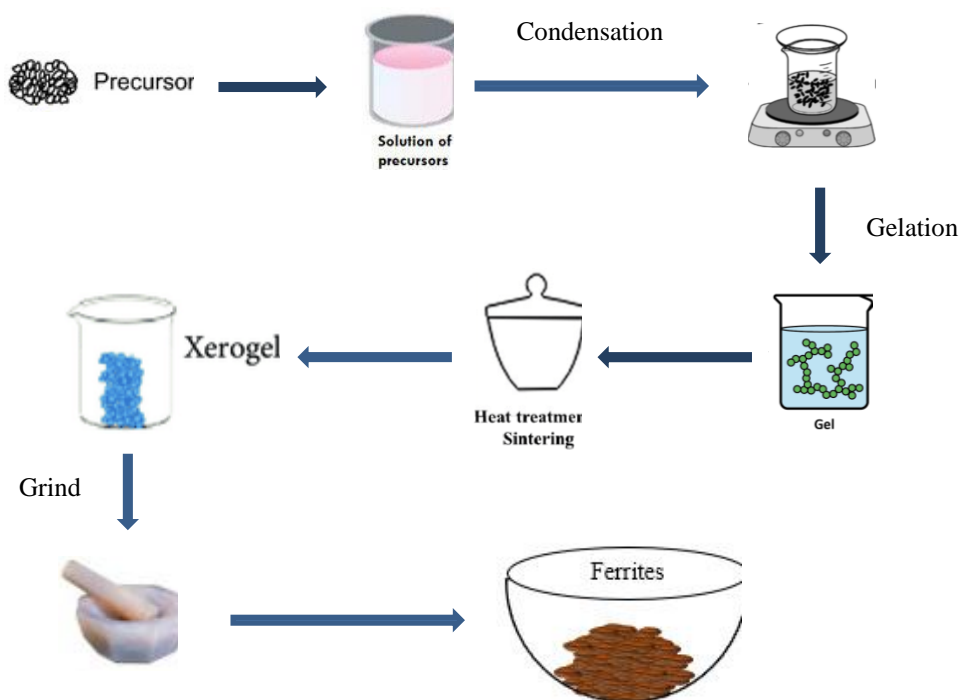


Figure 2. Synthesis process by Sol-Gel Method

2.2 Solid State Method

A wide range of materials, such as nitrides, sulfides, aluminosilicates and mixed metal oxides, can be manufactured using the traditional ceramic process. This synthesis method requires several steps, starting with the homogenization of two or more solid compounds, which is followed by grinding in a wet medium to control particle size and create a homogenous blend, compaction, and heating the mixture at a high temperature, as illustrated in Figure 3 [20,21].

Polycrystalline solids are frequently created from a mixture of solid reactants via solid-state processes. High temperatures are needed to start a reaction because mixtures of solids do not react at room temperature for very long (chemical breakdown of reactants). Surface area, reactivity, free energy change, and other chemical characteristics and morphological of the reactants all have an impact on these processes [22]. In addition to producing complicated oxides, these processes are used to make advanced materials such as piezoelectrics. To create a new solid alignment with gas development, physical mixing of simple oxides, nitrates, hydroxide, carbonate, alkoxides, oxalates, sulphate, or other metal salts is followed by high temperature treatment, typically between 1000°C and 1500°C [23]. Large-scale production of ferrite materials with a high yield and minimal pollution is possible through solid-state processes [24].

Chapter 4

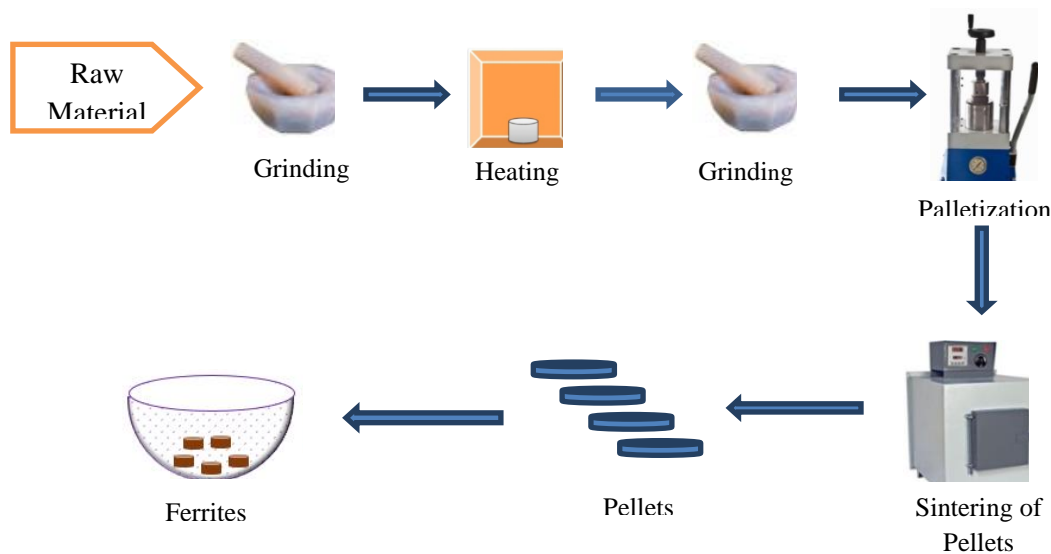


Figure 3. Synthesis process by solid state Method

2.3 co-precipitation method

The easiest and most practical way to create magnetic particles is by chemical co-precipitation. Using this method, two or more cations precipitate to produce a uniform composition [25]. Four steps make up this method: nucleation, growth, coarsening, and agglomeration all occur simultaneously [26]. The co-precipitation method involves introducing a mixture solution containing cation chloride (Fe, Sr, etc.) dropwise into a solution of NaOH/Na₂CO₃. This process produces precipitation. To create HFs, cations with carbonate or nitrate can be substituted for chloride cations. In contrast, hydrochloric acid transforms cations of carbonate, like SrCO₃, into cations of chloride in the latter scenario. After filtering and ethyl alcohol washing the precipitates until no NaCl is visible, the pH is maintained below 8. As illustrated in Figure 4, the cleaned precipitates are dried and calcined for three hours at 950 °C.

Some benefits of this approach include its simplicity, ease of controlling particle size, uniformity of small-sized nanomaterials, energy-efficient bulk production of magnetic nanoparticles, etc. The method's drawbacks include trace impurity, time consumption, and nanoparticle instability [26].

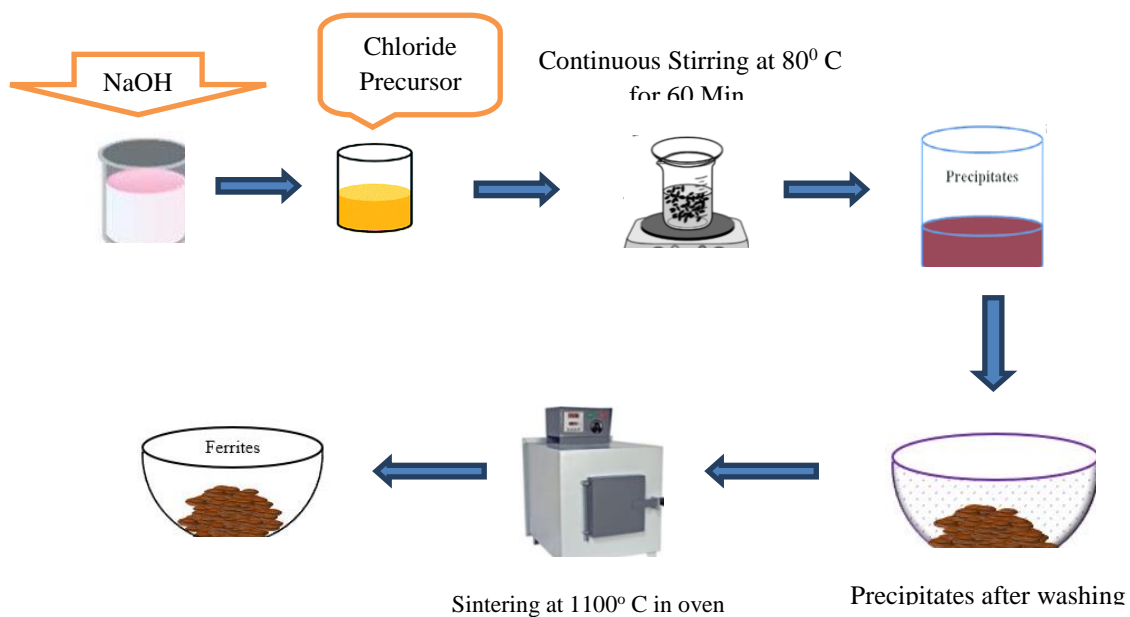


Figure 4. Synthesis process by co-precipitation Method



Chapter 4

3. CHARACTERIZATION NANO FERRITES

To look into structural, electrical, magnetic, and microwave absorption, characterization is done.

3.1 Structural Property

According to the XRD principle, constructive interference happens for a fixed set of incidence angle (θ) and interplanar spacing (d) for a given wavelength (λ). Bragg's has provided a mathematical equation that relates the incident X-ray wave length, the layer's distance, and the angle of diffraction [27].

$$2 d \sin \theta = n \lambda \quad (1)$$

where $n = (1, 2, 3, 4, \dots \text{etc.})$

The crystallite size can be calculated by Debye-Scherrer equation as follows [28].

$$D = \frac{0.9 \lambda}{\beta \cos \theta}$$

Where, D = Size of crystallite (in nm), β = full width at half maximum of the peak (in radians), λ = X ray wavelength ($\lambda = 1.5406 \text{ \AA}$), θ = Bragg's angle (in radians),

The lattice dimension (a) is calculated by following formula [29]

$$d = \frac{a}{\sqrt{h^2 + k^2 + l^2}}$$

Where, d = interplanar spacing and h, k and l are the miller indices.

The true density (X-ray density) is calculated by the relation which is given bellow [37]

$$D_x = \frac{Z M}{N_a a^3}$$

Where, M = Molecular weight of the sample, a =lattice constant, N =Avagadro number.

Now, the porosity (p) of the ferrite is can be calculated as follows [29]

$$p = 1 - \frac{D}{D_x}$$

Where, D = apparent density of the prepared sample

The real crystal structure, crystallite size and strain, long range order, porosity, phase identification, unit cell volume, etc. of ferrites are all ascertained by X-ray diffraction (XRD) [30, 31].

3.2 Scanning Electron Microscopy

SEM is used to examine the morphological properties of the resultant nano-ferrite. High-energy electrons are scanned across a ferrite surface to produce images [32]. These concentrated electrons interact with the different atoms in the ferrite to produce heat, visible light, secondary electrons, diffracted backscattered electrons, a characteristic X-ray, and other signals when they collide with the ferrite surface. It alludes to the investigation of ferrites' size, shape, and structure.

3.3 FTIR Spectroscopy

It is the technique that is most frequently used to identify the functional groups in Cd ferrites that are produced. In order to do this, the sample is exposed to an infrared radiation between 400 and 4000 cm^{-1} , and the molecular structure is ascertained by measuring the absorbance of these radiations by ferrite. Rather than often producing electrical excitation, infrared radiation produces vibration excitation, which causes the bond connecting atoms or groups of atoms to vibrate more quickly. Plotting the substance's absorbance of infrared light in contradiction of its wavelength, the FT-IR



spectrometer creates an IR spectrum [33]. Table 4 reports some of the ferrites tetrahedral bond and octahedral bond from FTIR Analysis

3.4 Vibrating sample magnetometer

Utilizing Faraday's principle of induction, a vibrating sample magnetometer (VSM) examines the magnetic properties of magnetic materials [34, 35]. In vector signal modulation (VSM), a fluctuating magnetic field generates an electric field, which provides information about the fluctuating magnetic field. Saturation magnetization, Hysteresis loop, remanence, coercivity, and magnetic moment can all be analyzed using VSM data [34, 35, 36]. Table 5 reports some of the ferrites magnetic properties from VSM Analysis

4. Conclusion

Ferrites' basic characteristics, research trend, properties, and classification were all covered. For the preparation of Nano ferrites, the most popular techniques— chemical co-precipitation, sol gel, and solid state methods—were contrasted. The XRD is used to calculate the structure, crystallite size, and properties of ferrites. The SEM micrographs demonstrated that substitutions and their doping percentage level have a significant impact on the microstructure development, morphology, and grain size. The formation of the nano ferrites with different dopant elements was confirmed by the FTIR study. The position of both bonds changed from their initial positions with distinct substitutions, can be calculated by the FTIR analysis. The impact of substitutions, grain size, doping percentage level, and temperature on the magnetic properties of ferrites was revealed by an insight into a vibrating sample magnetometer.

References

- [1] Adam JD, Davis LE, Dionne GF, et al. (2002) Ferrite devices and materials. *IEEE T Microw Theory* 50: 721–737.
- [2] Ajitanshu Vedrtmam, Kishor Kalauni, Sunil Dubey and Aman Kumar (2020) *Material Science: A comprehensive study on structure, properties, synthesis and characterization of ferrites*. *AIMS Material Science* 7: 800-835
- [3] Pullar RC (2012) Hexagonal ferrites: A review of the synthesis, properties and applications of hexaferrite ceramics. *Prog Mater Sci* 57: 1191–1334.
- [4] Santosh Bhukal, S. Bansal, Sonal Singhal, *Journal of Molecular Structure* 1059 (2014) 150–158
- [5] Arun Vijay Bagade, Pratik Arvind Nagwade, Arvind Vinayak Nagawade, Shankar Ramchandra Thopate And Sangita Nanasahab Pund, *A Review on Synthesis, Characterization and Applications of Cadmium Ferrite and its Doped Variants orient. J. Chem., Vol 38(1), 01-15 (2022)*
- [6] M.A. Yousuf, S. Jabeen, M.N. Shahi, M.A. Khan, I. Shakir, M.F. Warsi, *Results Phys.* 16 (2020) 102973.
- [7] Sickafus, K. E.; Wills, J. M.; Grimes, N. W. *J. Am. Ceram. Soc.*, **1999**, 82, 3279–3292.
- [8] Harpreet Kaur, Amrik Singh, Vijay Kumar, Dharamvir Singh Ahlawat *Structural, thermal and magnetic investigations of cobalt ferrite doped with Zn²⁺ and Cd²⁺ synthesized by auto combustion method Journal of Magnetism and Magnetic Materials* 474 (2019) 505–511
- [9] W. Zhongli, L. Xiaojuan, L. Minfeng, C. Ping, L. Yao, M. Jian, *J. Phys. Chem.* 112 B (2008) 11292.
- [10] V.S. Kumbhar, A.D. Jagadale, N.M. Shinde, C.D. Lokhande, *J. Appl. Surf. Sci* 259 (2012) 39.
- [11] Paramesh D, Kumar KV, Reddy PV (2016) Influence of nickel addition on structural and magnetic properties of aluminium substituted Ni–Zn ferrite nanoparticles. *Process Appl Ceram* 10: 161–167.
- [12] Singh S, Ralhan NK, Kotnala RK, et al. (2012) Nanosize dependent electrical and magnetic properties of NiFe₂O₄ ferrite. *IJPAP* 50: 739–743.
- [13] Nejati K, Zabih R (2012) Preparation and magnetic properties of nano size nickel ferrite particles using hydrothermal method. *Chem Cent J* 6: 23.
- [14] Melagiriappa E, Jayanna HS (2009) Structural and magnetic susceptibility studies of samarium substituted magnesium-zinc ferrites. *J Alloy Compd* 482: 147–150.
- [15] Lazarević ZŽ, Jovalekić Č, Sekulić D, et al. (2012) Characterization of nanostructured spinel NiFe₂O₄ obtained by soft mechanochemical synthesis. *Sci Sinter* 44: 331–339.



- [16] Gözüak F, Köseoğlu Y, Baykal A, et al. (2009) Synthesis and characterization of $\text{Co}_x\text{Zn}_{1-x}\text{Fe}_2\text{O}_4$ magnetic nanoparticles via a PEG-assisted route. *J Magn Magn Mater* 321: 2170–2177.
- [17] Peterson DS (2013) Sol-gel technique, In: Li D, *Encyclopedia of Microfluidics and Nanofluidics*, New York: Springer Science + Business Media, 1–7.
- [18] Muresan LM (2015) Corrosion protective coatings for Ti and Ti alloys used for biomedical implants, In: Tiwari A, Rawlins J, Hihara LH, *Intelligent Coatings for Corrosion Control*, Boston: Butterworth-Heinemann, 585–602.
- [19] Xu P (2001) Polymer-ceramic nanocomposites: ceramic phases, In: Buschow KHJ, Cahn RW, Flemings MC, et al., *Encyclopedia of Materials: Science and Technology*, Oxford: Elsevier, 7565–7570.
- [20] Šepelák V, Bergmann I, Feldhoff A, et al. (2007) Nanocrystalline nickel ferrite, NiFe_2O_4 : Mechanosynthesis, nonequilibrium cation distribution, canted spin arrangement, and magnetic behaviour. *J Phys Chem C* 111: 5026–5033.
- [21] Rao CNR, Biswas K (2015) Ceramic methods, *Essentials of Inorganic Materials Synthesis*, John Wiley & Sons, 17–21.
- [22] Cho, S. J.; Uddin, M. J.; Alaboina, P. “Emerging Nanotechnologies in Rechargeable Energy Storage Systems”, 2017, 83-129, doi:10.1016/b978-0-323-42977-1.00003-0.
- [23] Buekenhoudt, A.; Kovalevsky, A.; Luyten, Ir J.; Snijkers, F. Basic Aspects in Inorganic Membrane Preparation in “Comprehensive Membrane Science and Engineering”, 2010, 1, 217-252.
- [24] Dao-hua, L.; Shao-fen, H.; Jie, C.; Chengyan, J.; Cheng Y. *IOP Conf. Ser.: Mater. Sci. Eng.*, 2017, 242, 012023.
- [25] Liu S, Ma C, Ma MG, et al. (2019) Magnetic nanocomposite adsorbents, In: Kyzas GZ, Mitropoulos AC, *Composite Nanoadsorbents*, Elsevier, 295–316.
- [26] Rane AV, Kanny K, Abitha VK, et al. (2018) Methods for synthesis of nanoparticles and fabrication of nanocomposites, In: Bhagyaraj MS, Oluwafemi OS, Kalarikkal N, et al., *Synthesis of Inorganic Nanomaterials*, Woodhead Publishing, 121–139.
- [27] Chatterjee AK (2001) X-ray diffraction, In: Ramachandran VS, Beaudoin JJ, *Handbook of Analytical Techniques in Concrete Science and Technology: Principles, Techniques and Applications*, Norwich, New York: William Andrew Publishing, 275–332.
- [28] Kumar, C. G.; Pombala, S.; Poornachandra, Y.; Agarwal, S. V. *Nanobiomaterials in Antimicrobial Therapy, Applications of Nanobiomaterials.*, 2016, 6, 103-152.
- [29] Nikumbh, A. K.; Nagawade, A. V.; Gugale, G. S.; Chaskar, M. G.; Bakare; P. P. *J. Mater. Sci.*, 2002, 3(7), 637–647.
- [30] Moscoso-Londoño O, Tancredi PABLO, Muraca D, et al. (2017) Different approaches to analyze the dipolar interaction effects on diluted and concentrated granular superparamagnetic systems. *J Magn Magn Mater* 428: 105–118.
- [31] Liu Q, Liu Y, Wu C (2017) Investigation on Zn–Sn co-substituted M-type hexaferrite for microwave applications. *J Magn Magn Mater* 444: 421–425.
- [32] McMullan, D. *Scanning electron microscopy 1928-1965*, Scanning., 1995, 17, 175–185.
- [33] Silverstein, R.; Webster, F.; Kiemle, D., *Spectrometric Identification of Organic Compounds*, John Wiley and Sons Inc., New York., 2006.
- [34] Manju BG, Raji P (2018) Synthesis and magnetic properties of nano-sized $\text{Cu}_{0.5}\text{Ni}_{0.5}\text{Fe}_2\text{O}_4$ via citrate and aloe vera: A comparative study. *Ceram Int* 44: 7329–7333.
- [35] Dairy ARA, Al-Hmoud LA, Khatatbeh HA (2019) Magnetic and structural properties of barium hexaferrite nanoparticles doped with titanium. *Symmetry* 11: 732.
- [36] Nikumbh, A. K.; Nagawade, A. V.; Gugale, G. S.; Chaskar, M. G.; Bakare; P. P. *J. Mater. Sci.*, 2002, 3(7), 637–647.
- [37] Salma Ikram, Jolly Jacob, M.I. Arshad, K. Mahmood, A. Ali, N. Sabir, N. Amin, S. Hussain, Tailoring the structural, magnetic and dielectric properties of Ni-Zn- Cd Fe_2O_4 spinel ferrites by the substitution of lanthanum ions *Ceramics International* 45 (2019) 3563–3569